Biochemical Systematics and Ecology 56 (2014) 49–59

Contents lists available at ScienceDirect

Biochemical Systematics and Ecology

journal homepage: www.elsevier.com/locate/biochemsyseco

A range wide geographic pattern of genetic diversity and population structure of *Hexinia polydichotoma* (Asteraceae) in Tarim Basin and adjacent areas

Su Zhihao [a], Zhang Mingli [a,b,*]

[a] Key Laboratory of Biogeography and Bioresource in Arid Land, Xinjiang Institute of Ecology and Geography, Chinese Academy of Sciences, Urumqi 830011, China
[b] Institute of Botany, Chinese Academy of Sciences, Beijing 100093, China

ARTICLE INFO

Article history:
Received 10 December 2013
Accepted 17 April 2014
Available online

Keywords:
Hexinia polydichotoma
Genetic diversity
Evolutional process
Geographic pattern

ABSTRACT

In order to investigate the genetic diversity and influence of climate oscillations on evolutionary processes of organisms in northwest China, we selected *Hexinia polydichotoma*, a species endemic to China, and examined the geographic pattern of genetic variation in its entire cover range, Tarim Basin and adjacent areas. In the study, 22 chloroplast (cp) haplotypes were identified based on two cpDNA sequences (*trn*H–*psb*A and *ycf*6–*psb*M), and five ITS sequence variations were found. Shown in the cp haplotype network, the two common cp haplotypes mainly distributed along the northern and southern rims of the basin respectively and intersected in the center of the basin, whereas in the ITS network, ITS genotype 1 was widespread across the whole distribution area, and rare genotypes were concentrated in the western rim of the basin. Genetic variation primarily occurred among populations and SAMOVA groups. Fragmented desert habitat may have caused gene flow barrier among populations or groups far from each other, leading to significant genetic differentiation at these levels. It appears that expansion and contraction cycles of river systems and oases during the middle Pleistocene was the source of the observed fragmentation. Geographic range expansion in *H. polydichotoma* was supported by the significant value for Tajima's *D*, Fu's F_S, and by a unimodal mismatch distribution. It was possible that the enlargement of the Taklimakan Desert during the middle Pleistocene may have provided appropriate conditions for the range dispersal. We identified western rim of the basin as the center of genetic diversity of *H. polydichotoma* based on the present dataset.

1. Introduction

The Tarim Basin is the largest endorheic basin in China. It covers approximately 530,000 km^2, stretching 1400 km from east to west, and 520 km from north to south (Liu and Qin, 2005). The Taklimakan Desert, the world's second largest shifting-sand desert, locates in the center of the basin, occupying nearly 60% of its area (Liu and Qin, 2005). The basin is surrounded by

* Corresponding author. Institute of Botany, Chinese Academy of Sciences, Beijing 100093, China. Tel.: +86 991 7823152, +86 13691033072; fax: +86 991 7823151.
E-mail addresses: zhangml@ibcas.ac.cn, zhangml@ms.xjb.ac.cn (Z. Mingli).

http://dx.doi.org/10.1016/j.bse.2014.04.005
0305-1978/

high mountains on three sides, the Tian Shan mountains on the north, the Kunlun and Altun Mountains on the south, and the Pamir Plateau on the west. It is opened to the Hexi Corridor on the east. Glaciers have developed on many of the peaks of the surrounding mountains, and the melting glaciers feed the oases around the rim of the basin (Liu and Qin, 2005). Evidence from the eolianite sediments suggests that the Taklimakan Desert and the adjacent oases initially formed during the middle Pleistocene (Mu, 1994), whereas the hot and dry climate of the basin had developed earlier in the late Cretaceous (Liu and Qin, 2005; Mu, 1994), and was exacerbated during the late Tertiary, when the uplift of the Tibetan Plateau altered the atmospheric circulation in the basin (Zheng et al., 2003; Sun et al., 2008). Glacial–interglacial cycles in the Quaternary caused a serial effects upon basin environments; as the temperature of the basin rose or dropped, the water volume of the rivers increased or decreased, respectively, resulting in shifts in the size of the desert and its oases (Zhang et al., 2003).

There is some population genetic patterns of plant species have been studied in the basin and adjacent areas. For example, Wang et al., (2011a) found genetic differentiation and introgressions between two ecologically divergent poplar species, *Populus euphratica* Oliver and *Populus pruinosa* Schrenk, using different types of genetic markers, and Wang et al., (2011b) also found the high level of genetic diversity and low genetic differentiation between populations within *P. pruinosa*. Guo et al. (2010) found allopatric divergence and regional range expansion in *Juniperus Sabina*, and the similar pattern was also found in, *Reaumuria soongarica* (Li et al., 2012). Further phylogeographical studies of desert plants in northwest China are of interest to obtain a better understanding of the evolutionary response to Quaternary climate aridification and oscillations. For those endangered species or some plant resources suffering diseases, phylogeographical studies can also provide some conservation implications (Ge et al., 2011).

Hexinia is a monotypic genus endemic to China (Ling and Shi, 1997; Zhao and Zhu, 2003). It belongs to Lactucinae Less. in Cichorieae of Asteraceae (Ling and Shi, 1997), and preliminary data suggest that it is derived from *Chondrilla*, also a genus of Lactucinae Less. in Cichorieae of Asteraceae of the xerophilic Tethys flora (Ling and Shi, 1997; Yang, 1992). This perennial herb has branches resembling antler, and thus has esthetic value. It is tolerant to drought and salt, and therefore has value in resisting wind and fixing sand (Song et al., 2013). A powdery mildew was found to be seriously epidemic on *Hexinia polydichotoma* now (Song et al., 2013), from which it usually dies massively. Studying the geographic pattern of genetic variation of *Hexinia* can help in revealing factors that have shaped evolutional history and in determining conservation priorities for the species, whereas it is not fully understood by now.

Although the phylogeography of *H. polydichotoma* has been investigated using two chloroplast DNA (cpDNA) spacers, *ycf*6–*psb*M and *psb*A–*trn*H (Su et al., 2012), inferences on phylogeographical history of the species were not sufficiently supported, due to the limited variation displayed by the cpDNA markers, and because of the absence of sampling in the center of the Taklimakan Desert. Furthermore, cpDNA is usually inherited from only one of the parents (Birky, 2001; Xu, 2005), and so cpDNA markers may only partly recover the phylogeographical history of a species (Mäder et al., 2010). The additional use of biparentally inherited nuclear DNA markers might therefore contribute significantly to uncovering of the evolutionary history (Liu et al., 2012). Recently, the combination of nuclear and chloroplast markers used in plant population genetic studies has been increasingly (Jia et al., 2012; Takahashi et al., 2008; Martins et al., 2011). In the present study, we used both nuclear and chloroplast markers to investigate the full, range wide genetic variation of *H. polydichotoma* with specific aims to (1) estimate levels of genetic variation and population differentiation, (2) infer the demographical history of the species, (3) identify the center of genetic diversity across the populations.

2. Materials and methods

2.1. Sampling

A total of 326 individuals from 24 populations of *H. polydichotoma* were included in the present study. This sampling covers the entire geographic range of the species, including the Tarim Basin as well as its adjacent areas, the Turpan Basin and Hexi Corridor. Of the sampled populations, 19 are from the Tarim Basin, 2 are from the Turpan Basin, and 3 are from the Hexi Corridor. In each population, 7–20 individuals were collected, and from each, fresh stems and leaves were gathered and dried in silica gel. We selected one closely related species, *Chondrilla brevirostris*, as the outgroup of chloroplast haplotype phylogenic study, and we chose *Hyoseris radiata* as the outgroup of ITS network study (Zhang et al., 2011).

2.2. DNA extraction, amplification, and sequencing

Total genomic DNA was extracted from silica-gel-dried leaf tissue using a modified 29 CTAB method (Rogers and Bendich, 1985; Doyle and Doyle, 1987). The intergenic spacer *trn*H–*psb*A was amplified and sequenced using the primers and protocols of Sang et al., (1997), and the *ycf*6–*psb*M spacer was amplified and sequenced using the primers and protocols of Demesure et al., (1995). Amplification and sequencing of the ITS region (ITS1, 5.8S rDNA, ITS2) was originally performed with primers ITS1 and ITS4 (White et al., 1990). After successful amplification and sequencing in several *Hexinia* individuals, two new primers were designed for *Hexinia*. The sequences of forward and reverse primers were 5′-TTGAGATTGGCTTTAGGTC-3′ and 5′-CACAACAAGACGAGGGTAT-3′, respectively. Amplification products were purified using the PCR product purification kit (Shanghai SBS, Biotech Ltd., China), following protocols provided by the manufacturer. The forward and reverse primers of the amplification reactions were employed in the sequencing reactions, which were conducted with the DYEnamic ET Terminator Kit (Amersham Pharmacia Biotech). Sequencing occurred at the Shanghai Sangon Biological Engineering Technology &

Services Co., Ltd. (Shanghai, China), using an ABI-PRISM 3730 automatic DNA analyzer. Electropherograms were edited and assembled using SEQUENCHER 4.1 (Gene Codes, Ann Arbor, MI, USA). Sequences were aligned with CLUSTAL W (Thompson et al., 1994) and refined by visual inspection.

2.3. Molecular variability and demographic analysis

HAPLONST (http://www.pierroton.inra.fr/genetics/labo/Software/index.html) was used to estimate within-population diversity (h_S) and total gene diversity (h_T). In order to investigate the possibility of population subdivision, spatial analysis of molecular variance was performed using the program SAMOVA v.1.0 (Dupanloup et al., 2002) to define groups of populations (K) that are geographically homogeneous and genetically differentiated from each other, and the analysis was run for $K = 2–23$. Finally, the number of groups that maximizes the proportion of total genetic variance due to differences among groups of locations (F_{CT}) was retained as the best grouping of populations. Based on pairwise differences of the sequences, analysis of molecular variance (AMOVA) was employed to study the genetic structure of the species (Excoffier et al., 1992). To test for evidence of range expansions, Tajima's D and Fu's F_S statistics were calculated (Tajima, 1989; Fu, 1997; Jaeger et al., 2005; Smith and Farrell, 2005). A significant value for D or a significant, large, negative value for F_S may be the result of population expansion (Fu, 1997; Aris-Brosou and Excoffier, 1996; Tajima, 1996). In order to investigate hypotheses of demographic history in another manner, the mismatch distribution was also calculated. The shape of the mismatch distribution provides evidence of a sudden population expansion during the history of a species. A multimodal distribution usually suggests that populations are at demographic equilibrium, while a unimodal distribution indicates that populations have experienced a recent expansion (Slatkin and Hudson, 1991; Rogers and Harpending, 1992), and in order to test for significance, 10,000 permutations were performed. All expansion tests were implemented in ARLEQUIN v.3.01 (Excoffier et al., 2005). If the sudden expansion model was not rejected, we used the relationship $s = 2\ ut$ to estimate the expansion time (t) (Rogers and Harpending, 1992), where s is the total number of mutations, and u is the mutation rate per generation for the whole analyzed sequence. The value of u was calculated as $u = 2\ \mu kg$, where μ is the substitution rate per nucleotide site per year (s/s/y), k is the average sequence length of the analyzed DNA region, and g is the generation time in years. The cpDNA substitution rates for most angiosperm species have been estimated to vary between 1 and 3×10^{-9} substitutions per site per year (s/s/y) (Wolfe et al., 1987), while those for nrITS in shrubs and herbal plants vary between 3.46 and 8.69×10^{-9} s/s/y (Richardson et al., 2001). Given the uncertainties in these rate values, we used normal distribution priors with a mean of 2×10^{-9} and a SD of 6.080×10^{-10} for cpDNA, and a mean of 6.075×10^{-9} and a SD of 1.590×10^{-9} for ITS to cover these rate ranges within the 95% range of the distribution for our estimation of divergence times (Jia et al., 2012). The generation time of *H. polydichotoma* is one year.

2.4. Haplotype network analysis

Relationships among cpDNA and ITS genotypes were inferred using TCS v.1.21 software (Clement et al., 2000), which uses a statistical parsimony method to estimate ancestral or intermediate haplotypes, as described by Templeton et al., (1992). For

Table 1
Details of sample locations, sample size, and haplotype frequencies for 24 populations of *H. polydichotoma*. Figures in the parenthesis represent the number of the haplotypes.

Number	Location	Latitude (N)	Longitude (E)	Altitude (m)	cp Haplotype	ITS haplotype
1	JintaA	39°58′	98°55′	1242	A (13), B (2)	1 (10)
2	Guazhou	40°50′	96°03′	1219	C (10)	1 (10)
3	Tuokexun	42°52′	88°44′	0	A (15)	1 (10)
4	Kuerle	41°52′	85°42′	918	A (15)	1 (10)
5	Kuche	41°44′	83°43′	1060	A (16)	1 (10)
6	Akesu	40°44′	79°55′	1063	A (15)	1 (10)
7	Atushi	39°44′	76°12′	1295	A (10), F (1), J (2), K (2)	1 (7), 2 (3)
8	Shule	39°23′	75°58′	1290	A (6), D (6), E (2), H (2), O (4)	1 (2), 2 (6), 3 (2)
9	Yuepuhu	39°06′	77°02′	1183	A (3), D (5), N (8), O (4)	1 (7), 4 (3)
10	Yecheng	37°57′	77°13′	1320	D (15)	1 (8), 5 (2)
11	Pishan	37°35′	78°11′	1424	D (15)	1 (5), 5 (5)
12	Hetian	37°01′	80°18′	1378	D (12), P (1), Q (2)	1 (10)
13	Cele	36°58′	80°49′	1407	D (13), I (1), L (2), M (1)	1 (10)
14	Qiemo	38°08′	85°34′	1333	D (14), G (1)	1 (10)
15	Ruoqiang	39°00′	88°09′	889	D (18), I (1)	1 (10)
16	Yuli	41°28′	86°14′	888	A (12)	1 (10)
17	JintaB	39°56′	98°52′	1241	A (10)	1 (10)
18	Tahe	41°07′	84°25′	934	A (7), D (2), R (1)	1 (10)
19	TarimA	40°01′	84°16′	1008	A (2), D (8)	1 (10)
20	TarimB	39°01′	83°37′	1106	G (3), S (1), T (3)	1 (10)
21	Alear	40°17′	81°12′	1003	D (2), U (8)	1 (10)
22	TarimC	40°08′	81°01′	1028	V (10)	1 (10)
23	TarimD	39°31′	80°35′	1053	A (2), D (8)	1 (10)
24	Turpan	42°45′	89°18′	−131	A (10)	1 (10)

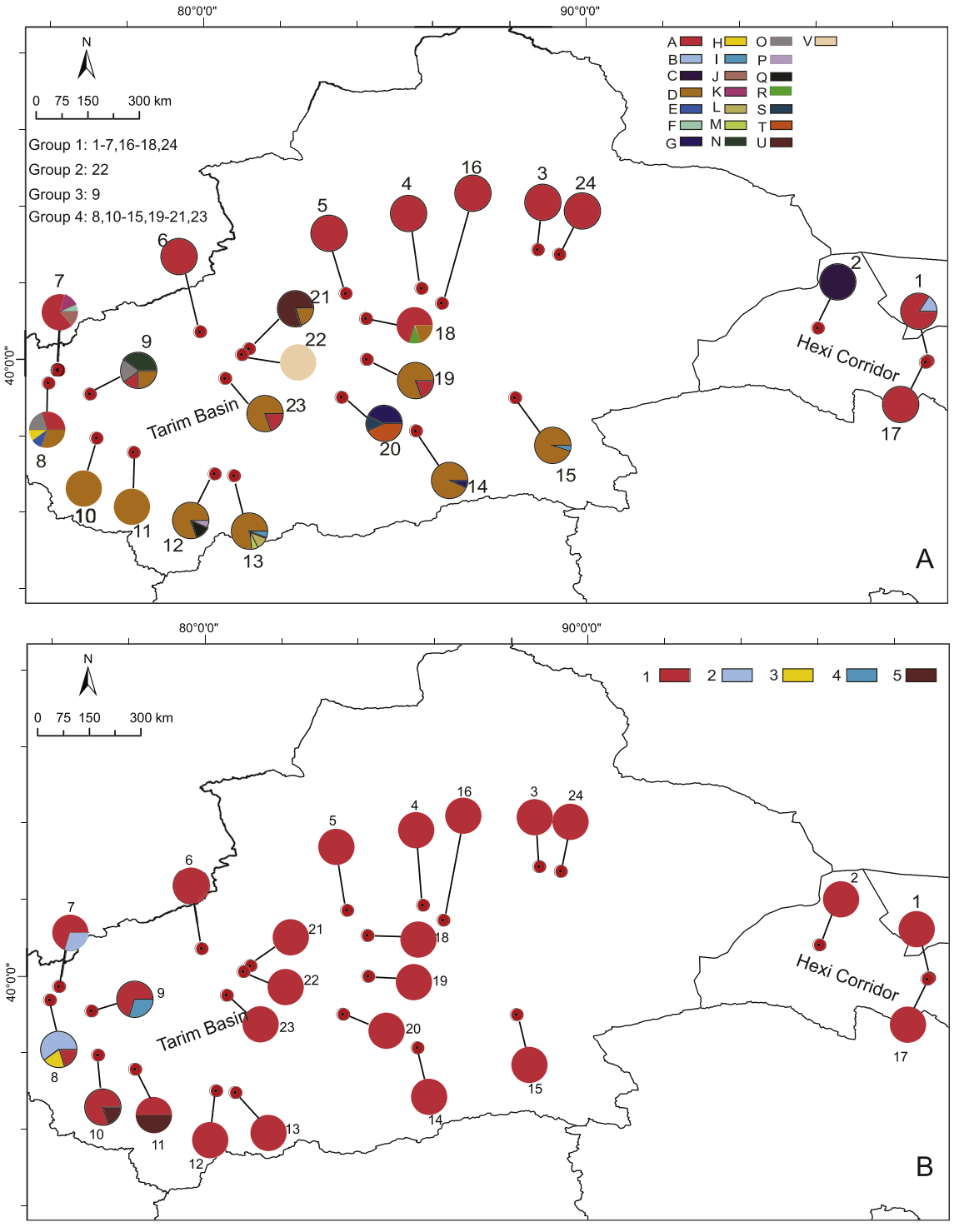

Fig. 1. The geographical distribution of (A) cp haplotype, and (B) ITS genotypes in *H. polydichotoma* in China. Population numbers correspond to those in Table 1; cp haplotypes to those in Table 2; ITS genotypes to those in Table 3.

cpDNA and ITS, we ran TCS with a default parsimony connection limit of 95%. After starting initially with the default limit (11 internal steps allowed), we added outgroup when fixing the connection limit at 168 and 76 steps respectively to link the divergent networks of the two species. Gaps (indels) detected in the cpDNA and ITS datasets were treated as single mutation events and coded as substitutions (A or T).

3. Results

3.1. Sequence analysis

The aligned sequence length for the *trn*H–*psb*A spacer was 530 base pairs (bp) and for the *ycf*6–*psb*M spacer is 600 bp. A total of 25 informative characters were found in the aligned sequence data: 17 nucleotide substitutions (positions 33, 56, 81, 110, 196, 306, 320, 348, 363, 370, 377, 443, 513, 894–897, 928, 984 and 1002) and eight indels (positions 65, 172–180, 222–231, 382–384, 385, 386–395, 799–804, and 867). Of the 326 sampled individuals from 24 populations, a total of 22 cp haplotypes (A–V) were identified (Tables 1 and 2). For the ITS region, the aligned sequence length was 490 bp, and 4 informative characters were found in the aligned sequence data, and they are all nucleotide substitutions (positions 191, 319, 400, 460). Of the 240 sampled individuals from 24 populations, 5 genotypes (1–5) were identified (Tables 1 and 3). GenBank accession numbers of the cpDNA sequences are JX183915-JX183936, KJ789147-KJ789150, and the ITS sequences accession numbers are KJ789151-KJ789155.

3.2. Haplotype geographical distribution and relationships

The geographic distribution of cp haplotypes, along with the frequency of haplotypes in each population, are presented in Fig. 1A, Table 1. In the network, cp haplotypes A and D are more widespread than the other haplotypes. Haplotype *A* is widespread along the western rim of the basin, northern rim of the basin, center of the basin, and Hexi Corridor. In contrast, haplotype D is widespread along the western rim of the basin, southern rim of the basin, and center of the basin. Haplotype A and D intersect in the center of the basin. Many rare haplotype, such as F, J, K, E, H, N, O, distributed in the western rim of the basin. At the southern rim of the basin, there are rare haplotypes such as I, G, P, Q, M, and L. In the center of the basin, there are special haplotypes such as R, S, T, U, and V. For ITS genotype, the common ITS genotype 1 appears in every population, and rare ITS genotypes such as 2, 3, 4, and 5, only appear in the western rim of the basin (Fig. 1B; Table 1).

The structure of the cp haplotype network demonstrates that some haplotypes may have direct or more distant relationships with others (Fig. 2). For example, haplotypes B, C, R, S, and N are connected to haplotype A by one substitution, while others are connected to it by more steps. Indeed, haplotype K is connected to A by two mutations, haplotype J is connected to K via three mutations, both haplotype F and U are connected to A by one mutation, and haplotype V is connected to A by 20 mutations. Haplotypes E, H, Q and T all connect to haplotype D by one step, while others, such as G, L, M, P, I, and O are connected to D by a greater number of steps. Haplotypes A connected to D via three mutations, resulting in a ring structure among haplotypes A, S, T, and D. For ITS region, genotypes 2, 3, 4, and 5 are all connected to genotype 1 by one substitution (Fig. 3).

Table 2
Twenty tow haplotypes of *H. polydichotoma* recognized on basis of two chloroplast DNA sequences, *trn*H–*psb*A and *ycf*6–*psb*M.

	Sequence position																							
Hap	33	56	65	81	110	172	196	222	306	320	348	363	370	377	382	385	386	443	513	799	867	894	928	1002
A	T	A	A	T	G	★	T	–	A	C	A	C	A	A	–	–	–	A	C	–	–	▼	T	A	T
B	T	A	–	T	G	★	T	–	A	C	A	C	A	A	–	–	–	A	C	–	–	▼	T	A	T
C	T	A	A	T	C	★	T	–	A	C	A	C	A	A	–	–	–	A	C	–	–	▼	T	A	T
D	T	A	A	T	G	★	T	–	A	C	A	C	A	A	–	–	–	A	C	–	–	▽	T	A	T
E	T	A	A	T	G	★	T	–	A	C	A	C	A	A	–	–	–	A	T	–	–	▽	T	A	T
F	G	A	A	T	G	★	T	–	C	C	A	C	A	A	–	–	–	A	C	–	–	▼	T	A	T
G	T	A	A	T	G	–	T	–	A	C	A	C	A	A	–	–	–	A	C	–	–	▽	T	A	T
H	T	A	A	T	G	★	T	–	A	C	A	C	A	A	–	–	–	A	C	–	–	▽	T	A	G
I	T	A	A	T	G	★	T	–	A	C	A	C	A	A	–	C	△	A	C	–	–	▽	T	A	T
J	T	G	A	T	G	★	T	–	A	C	A	C	C	A	–	–	–	A	C	–	–	▽	T	G	T
K	T	G	A	T	G	★	T	–	A	C	A	C	C	A	–	–	–	A	C	–	–	▼	T	G	T
L	T	A	A	G	G	★	T	◇	A	C	A	C	A	A	–	–	–	A	C	–	–	▽	T	A	T
M	T	A	A	T	G	★	T	◇	A	C	A	C	A	A	–	–	–	A	C	–	–	▽	T	A	T
N	T	A	A	T	G	★	T	–	A	C	A	C	A	A	–	–	–	C	C	–	–	▼	T	A	T
O	T	A	A	T	G	★	T	–	A	C	A	C	A	A	◆	T	△	A	C	–	–	▽	T	A	T
P	T	A	A	T	G	★	T	–	A	C	A	C	A	A	–	–	–	A	C	□	–	▽	T	A	T
Q	T	A	A	T	G	★	T	–	A	C	A	T	A	A	–	–	–	A	C	–	–	▽	T	A	T
R	T	A	A	T	G	★	T	–	A	C	A	C	A	T	–	–	–	A	C	–	–	▼	T	A	T
S	T	A	A	T	G	★	G	–	A	C	A	C	A	A	–	–	–	A	C	–	–	▼	T	A	T
T	T	A	A	T	G	★	G	–	A	C	A	C	A	A	–	–	–	A	C	–	–	▽	T	A	T
U	T	G	A	T	G	★	T	–	A	C	A	C	C	A	–	–	–	A	C	–	–	▽	T	A	T
V	T	A	A	T	G	★	T	–	A	T	C	C	A	A	–	–	–	A	C	–	⊕	▼	A	A	T

Hap: haplotype ★: AAATAACAA ◇: TATAAATTTG ◆: TTA △: TTATTACTTT □: GCTAAT ▼: TTTC ▽: GAAA ⊕: AACAGTAATAGAGAGTAT.

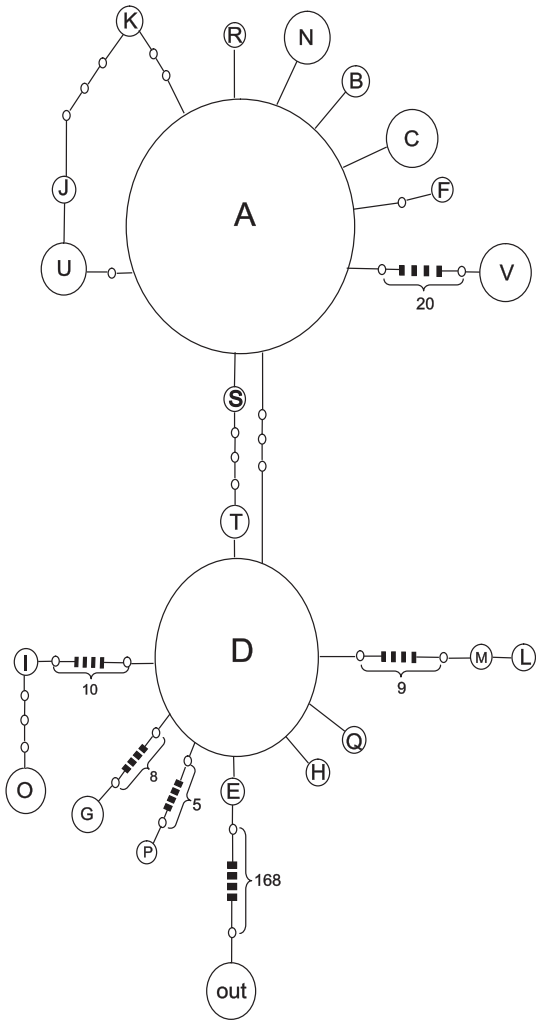

Fig. 2. cp Haplotype network of *H. polydichotoma* constructed under a criterion of statistical parsimony. The circle size is proportional to haplotype frequencies. The number of inferred steps between haplotypes is shown near the corresponding branch section. The blank dots represent the missing or inferred haplotypes.

3.3. Genetic diversity and genetic structure

Spatial genetic analysis of cpDNA haplotypes using SAMOVA indicated that F_{CT} increased to a maximal value of 0.6991 when K (the number of groups) was raised from $K = 2$ to $K = 4$. The grouping pattern of populations corresponding to $K = 4$ is:

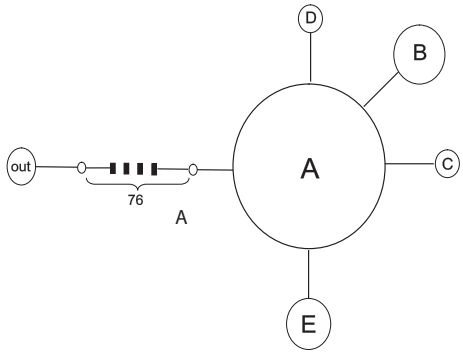

Fig. 3. ITS genotype network of *H. polydichotoma* constructed under a criterion of statistical parsimony. The circle size is proportional to genotype frequencies. The number of inferred steps between genotypes is shown near the corresponding branch section. The blank dots represent the missing or inferred genotypes.

Table 3
Five genotypes of *H. polydichotoma* recognized on basis of ITS sequences.

	Sequence position			
Genotype	1	3	4	4
	9	1	0	6
	1	9	0	0
1	C	C	G	G
2	C	C	G	A
3	C	C	T	G
4	A	C	G	G
5	C	T	G	G

(1) populations 1–7, 16–18, and 24 belonging to the northern rim of Tarim Basin and the Hexi Corridor; (2) population 22, belonging to the center basin; (3) population 9, belonging to the western rim of the basin; and (4) populations 8, 10–15, 19–21, and 23 belonging to the southern rim of the basin. Within-population gene diversity (h_S) was 0.236 (SE 0.0559), and total gene diversity (h_T) was 0.728 (SE 0.0539). Differentiation among populations was high ($G_{ST} = 0.676$, SE 0.0711), indicating population structure in *H. polydichotoma*. The AMOVA results provide evidence that 65.5% ($P < 0.001$) of the total variation can be explained by differences among populations. When populations were grouped according to geographical region, AMOVA results demonstrated that 69.9% ($P < 0.001$) of the total variation occurred among the groups (Table 4). For ITS sequences, within-population gene diversity (h_S) was 0.103 (SE 0.0427), and total gene diversity (h_T) was 0.168 (SE 0.0724). Differentiation among populations was high ($G_{ST} = 0.388$, SE 0.0491). The AMOVA results show that 34.2% ($P < 0.001$) of the total variation can be explained by differences among populations (Table 4).

3.4. Demographic analyses

Significant results of Tajima's *D*, Fu's *Fs*, along with unimodal distributions for the shapes of the mismatch distribution, suggest range expansions along the northern and southern rims of the basin (Fig. 4; Table 5). Based on the range of the cpDNA substitution rate, a haplotype sequence length of 1130 bp, and 1-year generation time, the time of the range expansion of *H. polydichotoma* is estimated to have occurred at about 0.44 million years (Mya), and based on the ITS substitution rate, the time of range expansion is about 0.25 Mya.

4. Discussion

4.1. Genetic diversity and genetic structure of H. polydichotoma

In *Hexinia*, a considerable high level of total genetic diversity as revealed by cp spacers ($h_T = 0.728$) might be explained by its wide geographic range. *H. polydichotoma* distributes in a large area of China, across the whole Tarim Basin which covers 530,000 km^2, and stretch eastern to the Hexi Corridor. Such vast distribution range should substantially contribute to the high level genetic diversity in the species. However, genetic differentiation among populations within group and within populations is low (Table 4), which suggests an absence of reproductive isolation among populations within groups and within populations of the study species. Lack of clear genetic structure among populations within groups could be explained by followed factors. First, *H. polydichotoma* can disperse far due to its abundant, small, and light fruits. This long dispersal distance will lead to limited genetic structure among populations (Palmé et al., 2003; Jones et al., 2006). Second, the terrain along the rim of the basin tends to be flat; therefore, unobstructed gene exchange may occur among populations. Opposite to low genetic differentiation among populations within group, there is moderately high genetic differentiation among the four

Table 4
Results of analysis of molecular variance for 24 populations of *H. polydichotoma* based on chloroplast DNA sequence data and ITS region.

Data set	Source of variation	d.f.	Sum of squares	Variance components	Percentage of variation (%)
cpDNA data	Among populations	23	530.785	1.6402	65.5*
	Within populations	302	260.783	0.8635	34.5
	(1–7, 16–18, 24) vs. (9) vs. (22) vs. vs. (8–15, 19–21, 23)				
	Among groups	3	467.326	2.4069	69.9*
	Among populations within groups	20	63.458	0.1727	5.0*
	Within populations	302	260.783	0.8635	25.1*
ITS region	Among populations	23	8.014	0.0295	34.2*
	Within populations	216	12.300	0.0569	65.8

* $P < 0.001$.

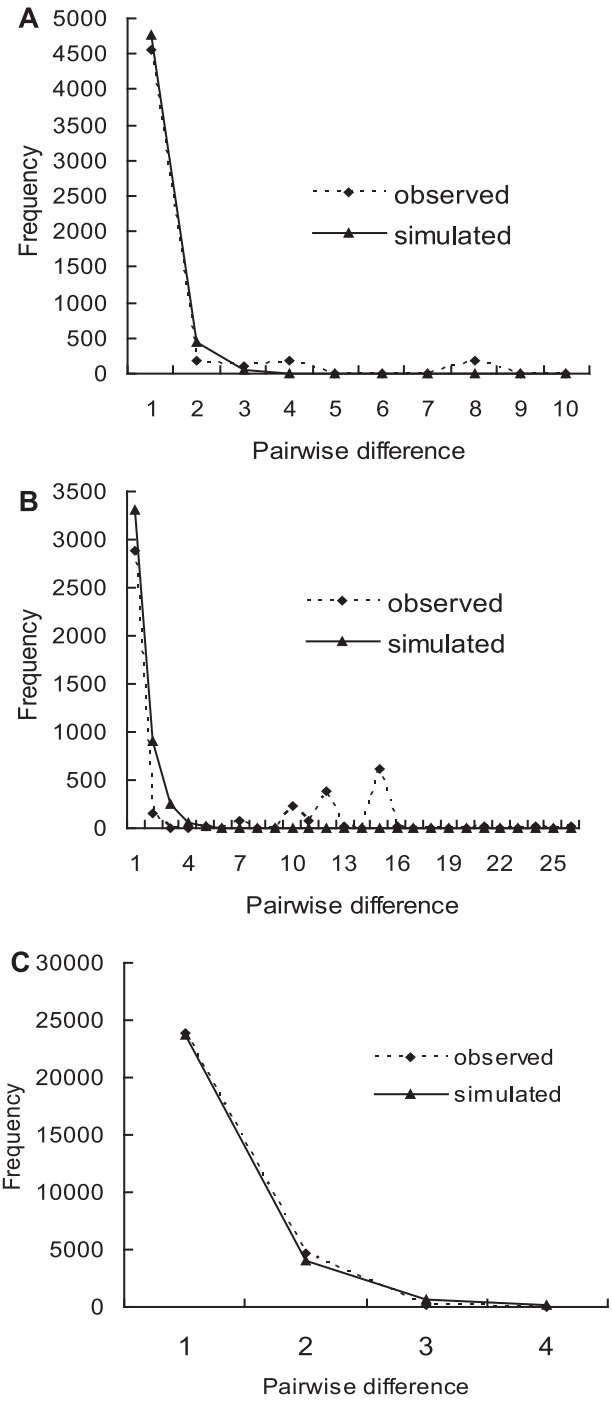

Fig. 4. Mismatch distribution analysis for chloroplast DNA data for (A) group (1) that includes populations 1–7, 16–18, and 24 (SSD = 0.0065, $P = 0.11$), (B) group (4) that includes populations 8, 10–15, 19–21, and 23 (SSD = 0.0671, $P = 0.06$), and (C) for ITS data (SSD = 0.0007, $P = 0.29$).

Table 5
Results of neutrality tests and mismatch distribution analysis for two groups and ITS region. Group (1) includes populations 1–7, 16–18, and 24, and group (4) includes populations 8–15, 19–21, and 23.

Data set	Group	τ	SSD (*P* value)	Hrag (*P* value)	Tajiam's *D* (*P* value)	Fu's *Fs* (*P* value)
cpDNA	Group (1)	3.00	0.0032 (0.39)	0.3658 (0.60)	−1.7900 (0.015)	−3.9293 (0.042)
Data	Group (4)	3.00	0.0671 (0.06)	0.4098 (0.59)	−1.2004 (0.073)	4.1390 (0.916)
ITS region	ITS	3.00	0.0007 (0.29)	0.4785 (0.75)	−1.2863 (0.044)	−4.1061 (0.017)

τ: time in number of generations elapsed since the sudden expansion episode; Hrag: the Harpending's Raggedness index; SSD: sum of squared deviations.

identified groups of *Hexinia* populations and among the populations (Table 4). Given that the fragmented desert habitat and the vast distributed area, groups or populations far from each other may have gene flow barrier. For ITS variation, the differences among populations is low, seemingly opposite to the results revealed by the cp spacers, and it may be explained by the low evolution rate in ITS region in this species. In northwest China, it is common that significant genetic differentiation between populations of the desert plants, such as *Pugionium cornutum* (Wang et al., 2013), *Juniperus Sabina* (Guo et al., 2010).

4.2. Genetic variation fragmentedly distributed in Tarim Basin and adjacent areas

Genetic variation fragmentation was an apparent characteristic in *Hexinia* genetic diversity. Haplotype A spread along the north rim of the basin, stretch to the center basin, and to the Hexi Corridor. The colonization of haplotype A is not continuous. In the diffused route of haplotype A, population 2, located between the northern rim and the Hexi Corridor, fixed the particular and highly derived haplotype C. Thought haplotype A and D intersect in the center of the basin, in the intersection route, population 22 fix a particular haplotype V. The same rare haplotype were found in distant populations, such as haplotypes I and G. Haplotype I is present in populations 13 and 15, and the distance between them is 721 km. Haplotype G is present in populations 14 and 20, and the distance between them is 400 km. We hypothesize that habitat fragmentation led to genetic variation fragmentedly distribution. Habitat fragmentation is a consequence of climate fluctuation throughout the basin. Though the arid climate has dominated the basin since the middle Pleistocene, climatic fluctuations have occurred frequently (Jin et al., 1994; Dong et al., 1997; Zhang and Men, 2002). From the middle Pleistocene to the Holocene, the climate of the Tarim Basin has cycled multiple times between dry and humid conditions, resulting in expansion and contraction cycles of river systems and oases (Zhang et al., 2003; Feng et al., 1999; Yang et al., 2002; Luo et al., 2009). These climatic shifts might have resulted in multiple rounds of habitat fragmentation, which has provided new opportunities for the colonization to different geographic areas. Processes resembling allopatric fragmentation of *H. polydichotoma* have been found in a number of other taxa in northwest China, such as *Juniperus sabina* (Guo et al., 2010), *Reaumuria soongarica* (Li et al., 2012), and *Nitraria sphaerocarpa* (Su and Zhang, 2013).

4.3. Range expansion in Tarim Basin and adjacent areas

Range expansion was detected in both cp spacers and ITS region. For cp spacers, the range expansion of group (1) was supported by the significant value of Tajima's *D* and Fu's F_S as well as by the unimodal mismatch distribution, and range expansion of group (4) was supported by the significant value of Tajima's *D* (Table 5, Fig. 4). For ITS region, range expansion of all population as a whole was supported by the significant value of Tajima's *D*, Fu's F_S, and unimodal mismatch distribution. In general, the migration patterns of individuals of *H. polydichotoma* have occurred along the rims of the basin, where the hydrographic net is well-developed and water is most abundant. Our results suggest that *H. polydichotoma* expanded between 0.25 and 0.44 Mya, which is during the middle Pleistocene (0.125–0.75 Mya) (Shi et al., 2005). Early in the Pleistocene, deserts were only scattered throughout the basin (Shi et al., 2005), but when the region became drier during the late-early or early-middle Pleistocene, the Taklimakan Desert and its migratory dunes formed (Shi et al., 2005). The drifting sand and wind may have provided appropriate conditions for the dispersal of *H. polydichotoma*. Geographic range expansions of this nature also have been reported in species in Europe, North America, and northeast Asia (Hewitt, 2000; Broyles, 1998; Aizawa et al., 2009), and also have been reported in *Juniperus sabina* (Guo et al., 2010), *Reaumuria soongarica* (Li et al., 2012), distributed in desert in northwest China.

4.4. The center of genetic diversity of H. polydichotoma

For both ITS region and cp spacers, there are unique haplotypes or genotypes and high levels of genetic variation were found in populations 7, 8, and 9. In population 8, there is ancestral cp haplotype E (Fig. 2), and in populations 10 and 11, there are also unique ITS genotypes 5. All these populations located in the western rim of the basin. According to Taberlet and Cheddadi, (2002), locations with high levels of genetic variation and unique haplotypes were examined as possible sites of refugia, or as a diversification center for the species, whereas locations with low levels of genetic variation were examined as possible sites of recent colonization. In our study, evidence above show the western rim of the basin included populations 7–11 must have played key roles as center of genetic diversity for *H. polydichotoma*. This result was in agreement with the study of Ma et al., (2012), in which the western area of Tarim Basin was pointed out to be a refugium or the center of genetic diversity of the *Gymnocarpos przewalskii* during the LGM. The other case is Yarkand hare, a species with a widespread distribution in the Tarim Basin, its refugium is also at the western rim of the basin (Shan et al., 2011). In the western rim of Tarim Basin, Tian Shan Mountains and Kunlun Mountains joins and consequently produces complicated topography (Mu, 1994), so we speculate it may provide favorable conditions for taking refugium or breeding high genetic diversity for *H. polydichotoma*. For the high genetic diversity in the populations located at the western rim of the basin, we suggest that they should be conserved preferentially.

In conclusion, we found significant genetic differentiation between populations in *H. polydichotoma*, and similar with other desert plants, we also found allopatric fragmentation and regional range expansion in *H. polydichotoma*, at last, we identified the center of genetic diversity of *H. polydichotoma*. However, whether the ITS variations may suggest interspecific hybridizations should be treated as a caveat in the present paper and need further examination in future.

Acknowledgements

This study is financially supported by China National Key Basic Research Program (2014CB954201) of Xinjiang Institute of Ecology and Geography, Chinese Academy of Science. We thank Stewart C. Sanderson at Shrub Sciences Laboratory, Intermountain Research Station, Forest Service, US Department of Agriculture, Utah 84601, USA, for his kind help in modifying the English language of the manuscript. We thank the anonymous reviewers for their helpful comments.

References

Aizawa, M., Yoshimaru, H., Saito, H., Katsuki, T., Kawahara, T., Kitamura, K., Shi, F., Sabirov, R., Kaji, M., 2009. Range-wide genetic structure in a north-east Asian spruce (*Picea jezoensis*) determined using nuclear microsatellite markers. J. Biogeogr. 36, 996–1007.
Aris-Brosou, S., Excoffier, L., 1996. The impact of population expansion and mutation rate heterogeneity on DNA sequence polymorphism. Mol. Biol. Evol. 13, 494–504.
Birky Jr., C.W., 2001. The inheritance of genes in mitochondrial and chloroplast: laws, mechanisms, and models. Annu. Rev. Genet. 35, 125–148.
Broyles, S.B., 1998. Postglacial migration and the loss of allozyme variation in northern population of *Asclepias exaltata* (Asclepiadaceae). Am. J. Bot. 85, 1091–1097.
Clement, M., Posada, D., Crandall, K.A., 2000. TCS: a computer program to estimate gene genealogies. Mol. Ecol. 9, 1657–1659.
Demesure, B., Sodzi, N., Petit, R.J., 1995. A set of universal primers for amplification of polymorphic non-coding regions of mitochondrial and chloroplast DNA in plants. Mol. Ecol. 4, 129–131.
Doyle, J.J., Doyle, J.L., 1987. A rapid DNA isolation procedure from small quantities of fresh leaf tissues. Phytochem. Bull. 19, 11–15.
Dong, G.R., Chen, H.Z., Wang, G.Y., Li, X.Z., Shao, Y.J., Jin, J., 1997. The evolution of deserts with climatic changes in China since 150 ka BP. Sci. China Ser. D. Earth Sci. 40, 370–382.
Dupanloup, I., Schneider, S., Excoffier, L., 2002. A simulated annealing approach to define the genetic structure of populations. Mol. Ecol. 11, 2571–2581.
Excoffier, L., Smouse, P., Quattro, J., 1992. Analysis of molecular variance inferred from metric distances among DNA haplotypes: applications to human mitochondrial DNA restriction data. Genetics 131, 479–491.
Excoffier, L., Laval, G., Schneider, S., 2005. Arlequin (version 3.0): an integrated software package for population genetics data analysis. Evol. Bioinforma. 1, 47–50.
Feng, Q., Su, Z.Z., Jin, H.J., 1999. Desert evolution and climatic changes in the Tarim River Basin since 12 ka BP. Sci. China Ser. D. Earth Sci. 42, 101–112.
Fu, Y.X., 1997. Statistical tests of neutrality of mutations against population growth, hitchhiking, and background selection. Genetics 147, 915–925.
Ge, X.J., Hwang, C.C., Liu, Z.H., Huang, C.C., Huang, W.H., Hung, K.H., Wang, W.K., Chiang, T.Y., 2011. Conservation genetics and phylogeography of endangered and endemic shrub *Tetraena mongolica* (Zygophyllaceae) in Inner Mongolia, China. BMC Genet. 12, 1.
Guo, Y.P., Zhang, R., Chen, C.Y., Zhou, D.W., Liu, J.Q., 2010. Allopatric divergence and regional range expansion of *Juniperus sabina* in China. J. Syst. Evol. 48, 153–160.
Hewitt, G.M., 2000. The genetic legacy of the Quaternary ice ages. Nature 405, 907–913.
Jaeger, J.R., Riddle, B.R., Bradford, D.F., 2005. Cryptic neogene vicariance and Quaternary dispersal of the red-spotted toad (*Bufo punctatus*): insights on the evolution of North American warm desert biotas. Mol. Ecol. 14, 3033–3048.
Jia, D.R., Abbott, R.J., Liu, T.L., Mao, K.S., Bartish, I.V., Liu, J.Q., 2012. Out of the Qinghai–Tibet Plateau: evidence for the origin and dispersal of Eurasian temperate plants from a phylogeographic study of *Hippophaë rhamnoides* (Elaeagnaceae). New. Phytol. 194, 1123–1133.
Jin, H.L., Dong, G.R., Jin, J., Li, B.S., Shao, Y.J., 1994. Environmental and climatic changes in the interior of Taklimakan Desert since Late Glacial Age. J. Desert Res. 14, 31–37 (in Chinese with English abstract).
Jones, M.E., Shepherd, M., Henry, R.J., Delves, A., 2006. Chloroplast DNA variation and population structure in the widespread forest tree, *Eucalyptus grandis*. Conserv. Genet. 7, 691–703.
Ling, R., Shi, Z., 1997. Asteraceae. In: Wu, Z.Y., Raven, P.H. (Eds.), Flora of China, vol. 80. Science Press, Beijing.
Li, Z.H., Chen, J., Zhao, G.F., Guo, Y.P., Kou, Y.X., Ma, Y.Z., Wang, G., Ma, X.F., 2012. Response of a desert shrub to past geological and climatic change: a phylogeographic study of *Reaumuria soongarica* (Tamaricaceae) in western China. J. Syst. Evol. 50, 351–361.
Liu, J.Q., Qin, X.G., 2005. Evolution of the environmental framework and oasis in the Tarim Basin. Quat. Sci. 25, 533–539 (in Chinese with English abstract).
Liu, J.Q., Sun, Y.S., Ge, X.J., Gao, L.M., Qiu, Y.X., 2012. Phylogeographic studies of plants in China: advances in the past and directions in the future. J. Syst. Evol. 50, 267–275.
Luo, C., Peng, Z.C., Yang, D., Liu, W.G., Zhang, Z.F., He, J.F., Chou, C.L., 2009. A lacustrine record from Lop Nur, Xinjiang, China: implications for paleoclimate change during Late Pleistocene. J. Asian Earth Sci. 34, 38–45.
Martins, K., Chaves, L., Vencovsky, R., Kageyama, P., 2011. Genetic structure based on nuclear and chloroplast microsatellite loci of *Solanum lycocarpum* A. St. Hil. (Solanaceae) in Central Brazil. Genet. Mol. Res. 10, 665–677.
Ma, S.M., Zhang, M.L., Sanderson, S.C., 2012. Phylogeography of the rare *Gymnocarpos przewalskii* (Caryophyllaceae): indications of multiple glacial refugia in north-western China. Aust. J. Bot. 60, 20–31.
Mäder, G., Zamberlan, P.M., Fagundes, N.J.R., Magnus, T., Salzano, F.M., Bonatto, S.L., Freitas, L.B., 2010. The use and limits of ITS data in the analysis of intraspecific variation in *Passiflora* L. (Passifloraceae). Genet. Mol. Biol. 33, 99–108.
Mu, G.J., 1994. On the age and evolution of the Taklimakan Desert. Arid. Land Geogr. 17, 1–9 (in Chinese with English abstract).
Palmé, A.E., Semerikov, V., Lascoux, M., 2003. Absence of geographical structure of chloroplast DNA variation in sallow, *Salix caprea* L. Heredity 91, 465–474.
Richardson, J.E., Pennington, R.T., Pennington, T.D., Hollingsworth, P.M., 2001. Rapid diversification of a species-rich genus of neotropical rain forest trees. Science 293, 2242–2245.
Rogers, S.O., Bendich, A.J., 1985. Extraction of DNA from milligram amounts of fresh, herbarium and mummified plant-tissues. Plant Mol. Biol. 5, 69–76.
Rogers, A., Harpending, H., 1992. Population growth makes waves in the distribution of pairwise genetic differences. Mol. Biol. Evol. 9, 552–569.
Sang, T., Crawford, D.J., Stuessy, T.F., 1997. Chloroplast DNA phylogeny, reticulate evolution, and biogeography of *Paeonia* (Paeoniaceae). Am. J. Bot. 84, 1120–1136.
Shan, W.J., Liu, J., Yu, L., Robert, W.M., Mahmut, H., Zhang, Y.P., 2011. Genetic consequences of postglacial colonization by the endemic Yarkand hare (*Lepus yarkandensis*) of the arid Tarim Basin. Chin. Sci. Bull. 56, 1370–1382.
Shi, Y.F., Cui, Z.J., Su, Z., 2005. The Quaternary glaciations and environmental variations in China. Hebei Science and Technology Publishing House, Hebei, 71–78.
Slatkin, M., Hudson, R.R., 1991. Pairwise comparisons of mitochondrial DNA sequences in stable and exponentially growing populations. Genetics 129, 555–562.
Smith, C.I., Farrell, B.D., 2005. Range expansions in the flightless longhorn cactus beetles, *Moneilema gigas* and *Moneilema armatum*, in response to Pleistocene climate changes. Mol. Ecol. 14, 1025–1044.
Song, J.G., He, G., Xu, B., Zhao, Z.Y., 2013. A powdery mildew fungus parasitizing sand binder *Hexinia Polydichotoma*. Mycosystema 32, 131–135.
Su, Z.H., Zhang, M.L., 2013. Evolutionary response to Quaternary climate aridification and oscillations in northwestern China revealed by chloroplast phylogeography of Nitraria sphaerocarpa (Nitrariaceae). Biol. J. Linn. Soc. 109, 757–770.
Su, Z.H., Zhang, M.L., Cohen, J.I., 2012. Phylogeographic and demographic effects of Quaternary climate oscillations in *Hexinia polydichotoma* (Asteraceae) in Tarim Basin and adjacent areas. Plant Syst. Evol. 298, 1767–1776.

Sun, J.M., Zhang, L.Y., Deng, C.L., Zhu, R.X., 2008. Evidence for enhanced aridity in the Tarim Basin of China since 5.3 Ma. Quat. Sci. Rev. 27, 1012–1023.
Taberlet, P., Cheddadi, R., 2002. Quaternary refugia and persistence of biodiversity. Science 297, 2009–2010.
Tajima, F., 1989. Statistical method for testing the neutral mutation hypothesis by DNA polymorphism. Genetics 123, 585–595.
Tajima, F., 1996. The amount of DNA polymorphism maintained in a finite population when the neutral mutation rate varies among sites. Genetics 143, 1457–1465.
Takahashi, T., Tani, N., Niiyama, K., Yoshida, S., Taira, H., Tsumura, Y., 2008. Genetic succession and spatial genetic structure in a natural old growth *Cryptomeria japonica* forest revealed by nuclear and chloroplast microsatellite markers. For. Ecol. Manag. 255, 2820–2828.
Templeton, A.R., Crandall, K.A., Sing, C.F., 1992. A cladistic analysis of phenotypic associations with haplotypes inferred from restriction endonuclease mapping and DNA-sequence data. 3. Cladogram estimation. Genetics 132, 619–633.
Thompson, J.D., Higgins, D.G., Gibson, T.J., 1994. Clustal-W—improving the sensitivity of progressive multiple sequence alignment through sequence weighting, position-specific gap penalties and weight matrix choice. Nucleic Acids Res. 22, 4673–4680.
Wang, J., Li, Z.J., Guo, Q.H., Ren, G.P., Wu, Y.X., 2011a. Genetic variation within and between populations of a desert poplar (*Populus euphratica*) revealed by SSR markers. Ann. For. Sci. 68, 1143–1149.
Wang, J., Wu, Y.X., Ren, G.P., Guo, Q.H., Liu, J.Q., Lascoux, M., 2011b. Genetic differentiation and delimitation between ecologically diverged *Populus euphratica* and *P. pruinosa*. PLoS ONE 6, e26530.
Wang, Q., Abbott, R.J., Yu, Q.S., Lin, K., Liu, J.Q., 2013. Pleistocene climate change and the origin of two desert plant species, *Pugionium cornutum* and *Pugionium dolabratum* (Brassicaceae), in northwest China. New. Phytol. 199, 277–287.
White, T.J., Bruns, T., Lee, S., Taylor, J.W., 1990. Amplification and direct sequencing of fungal ribosomal RNA genes for phylogenetics. In: Innis, M.A., Gelfand, D.H., Sninsky, J.J., White, T.J. (Eds.), PCR Protocols: a Guide to Methods and Applications. Academic Press, San Diego, pp. 315–322.
Wolfe, K.H., Li, W.H., Sharp, P.M., 1987. Rates of nucleotide substitution vary greatly among plant mitochondrial, chloroplast, and nuclear DNAS. Proc. Natl. Acad. Sci. U S A 84, 9054–9058.
Xu, J., 2005. The inheritance of organelle genes and genomes: patterns and mechanisms. Genome. 48, 951–958.
Yang, X.P., Zhu, Z.D., Jaekel, D., Owen, L.A., Han, J.M., 2002. Late Quaternary palaeoenvironment change and landscape evolution along the Keriya River, Xinjiang, China: the relationship between high mountain glaciation and landscape evolution in foreland desert regions. Quat. Int. 97–98, 155–166.
Yang, X.L., 1992. Flora of Desert from China. Science Press, Beijing.
Zhang, H.Y., Men, G.F., 2002. Stratigraphic subdivision and climatic change of the Quaternary of the center Taklimakan Desert. Xinjiang Geol. 20, 256–261 (in Chinese with English abstract).
Zhang, J.W., Nie, Z.L., Wen, J., Sun, H., 2011. Molecular phylogeny and biogeography of three closely related genera, *Soroseris, Stebbinsia*, and *Syncalathium* (Asteraceae, Cichorieae), endemic to the Tibetan Plateau, SW China. Taxon 60, 15–26.
Zhao, Y.Z., Zhu, Z.Y., 2003. The endemic genera of desert region in the centre of Asia. Acta Bot. Yunnanica 25, 113–121.
Zhang, H., Wu, J.W., Zheng, Q.H., Yu, Y.J., 2003. A preliminary study of oasis evolution in the Tarim Basin, Xinjiang. China J. Arid. Environ. 55, 545–553.
Zheng, H.B., Powell, C.M., Butcher, K., Cao, J.J., 2003. Late Neogene loess deposition in southern Tarim Basin: tectonic and palaeoenvironmental implications. Tectonophysics 375, 49–59.